Final Report for AASERT Program N00014-94-1-0726, "Nondestructive 3-Dimensional X-ray Diffraction Tomography of Stress/Strain Distribution around Fatigue Cracks in Al-Li 2090."

Stuart R. Stock
Associate Professor
School of Materials Science and Engineering
Georgia Institute of Technology
Atlanta, Georgia 30332-0245

A number of US citizens were supported during the three years of this program. In the first year, Mr. Curtis Patterson II was working on his MS, and Mr. Jake Haase and Ms. Victoria Snyder were employed as undergraduate assistants. In year two, Mr. Patterson left Tech to take a job with Pratt and Whitney (before finishing his thesis, he may defend it in March 1998) and Mr. Haase became a graduate student in this program, Three US citizens' graduate work was supported in the third year: Mr. J.D. Haase, Mr. J.R. Witt (2 quarters) and Mr. George Butler. The first two students concentrated on microtexture measurements in Al-Li 2090 T8E41 while the third followed a tangential line investigation on microtexture development within grains in copper samples after complex loading histories. Mr. Witt took a job with Boeing in June 1997, Mr. Butler will finish his PhD in March, 1998 and Mr. Haase will leave in December 1997 to found a CNC machining company. Three US citizens have been employed as undergraduate research assistants: Mr. Justin Clark, Ms. Stephanie Sprague and Mr. Tony Watt. All three are currently enrolled in the School, although Justin has begun MS work.

Research during the first year focused on making x-ray diffraction microbeam measurements routine. The principle focus was on how well microtexture from the outer and center parts of intact, full-sized plates of Al-Li 2090 could be separated by recording the pattern of diffracted intensity recorded on a two-dimensional detector as a function of increasing sample-detector separation. The model sample consisted of two 1 mm thick pieces sectioned parallel to the surface of a plate of Al-Li 2090. Plate one was from the surface and plate five was from the center of the plate, the plates spaced 3 mm apart and the x-ray beam was at normal incidence. As has been discussed by NRL researchers, there are two very different textures at these depths. The ray tracing approach allows one to determine within which of the plates diffracted streaks originated.

Research during the second year of this program continued using synchrotron polychromatic microbeams to map microtexture in three-dimensions in Al-Li 2090. Development of the novel techniques required for three-dimensional mapping and assessment of the precision of these techniques has been the major activity. The experiments which were part of this effort were concentrated on microbeam mapping on a number of compact tension samples. Beam diameters of 1 mm, 100 μm and 30 μm were used to examine samples in which fatigue cracks had already been propagated. Several samples without side-grooves were characterized before and after crack propagation. Most of microbeam mapping was done with the beam incident normal to the samples' faces, but some work was done at a series of inclinations up to 60° from the normal to
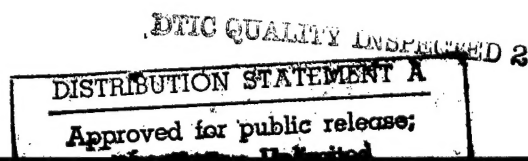
the surface. The angular distribution of diffracted intensity was recorded on reusable image storage plates because the mapping is much more rapid than with film due to the storage plates' far greater sensitivity and the shorter time required to process each diffraction pattern and because storage plates have several decades greater linear range than film. The model experiment developed to explore how well one can separate the contributions from adjacent volume elements (i.e., 40 μm thick grains in Al-Li 2090) showed considerable problems remained with the approach; these experiments continued into the third year. A wedge-shaped piece was sectioned parallel to the surface of and from the center of a plate of Al-Li 2090. Data consisted of the pattern of diffracted intensity recorded on a two-dimensional detector and its changes with increasing sample-detector separation. Analysis of this data is presently underway, and image readout with 0.05 mm pixels improved the precision with which the measurements could be made.

Research during the third of this program continued using synchrotron polychromatic microbeams to map microtexture in three-dimensions in Al-Li 2090. Mapping with a 0.01 mm diameter collimator became rapid and routine. There were two very important advances made during the past year and both have been communicated to the community in a recent national meeting presentation and in two manuscripts submitted for peer review. First, through x-ray microbeam diffraction mapping, the center portions of plates of Al-Li 2090 T8E41 were found to consist, to a significant degree, of regions where the grains were so highly oriented that they might be accurately termed near-single-crystalline. The centers of these plates are well known to have a very sharp, well developed average texture or macrotexture, but the extent to which these grains are clustered together and the extent to which the material consists of these quite large, discrete regions does not appear to have noted previously. Identification of this type of "mesotexture" appears to an important clue in efforts to improve fatigue prediction methodologies for a wide range of alloy systems.

The second main advance in the third year is that transitions in microtexture were correlated with asperity formation in samples fatigued under R=0.1 ($\sigma_{min}/\sigma_{max}$). Preliminary analysis of x-ray microbeam data collected during the past year for several cracked samples may provide guidance to improving the isotropy of mechanical properties of Al-Li 2090 T8E41. A near final draft is attached to summarize our current understanding, and it be submitted to Acta Mat within about one week.

In research somewhat tangential to the main effort under this program, the microbeam techniques were found to provide a rapid method of quantifying the amount of microtexture on the subgrain level from copper samples which underwent complex loading histories. Quantifying this subgrain microtexture is important to understanding why the various numerical models of texture evolution predict much sharper textures than are observed experimentally. This very exciting work indicates that the x-ray microbeam diffraction mapping of texture can be done at a synchrotron radiation source. We have demonstrated that data for the range of orientations within ten or more grains can be acquired within a couple of hours in a form which allows direct interpretation. A minimum of sample preparation is required, opening the possibility of observing the same collection of grains throughout their evolution. The information provided is roughly equivalent to that obtained through time-consuming transmission electron microscopy or through orientation imaging microscopy with a scanning electron microscope.

GRANT NUMBER: N00014-94-1-0726

FORM A2-2

JGMENTATION AWARDS FOR SCIENCE & ENGINEERING RESEARCH TRAINING (AASERT)
REPORTING FORM

e Department of Defense (DOD) requires certain information to evaluate the
fectiveness of the AASERT program. By accepting this Grant Modification,
ch bestows the AASERT funds, the Grantee agrees to provide the information
quested below to the Government's technical point of contact by each annual
niversary of the AASERT award date.

Grantee identification data: (R & T and Grant numbers found on Page 1 of Grant)

a. _Georgia Institute of Technology_
University Name

b. _N00014-94-1-0726_   c. _met 00a1--- 01_
Grant Number   - R & T Number

d. _Stuart R. Stock_   e. From: _7/1/96_ To: _9/30/97_
P.I. Name   AASERT Reporting Period

Grant to which AASERT award is attached is referred to hereafter as "Parent Agreement."

Total funding of the Parent Agreement and the number of full-time
ivalent graduate students (FTEGS) supported by the Parent Agreement during
12-month period **prior to** the AASERT award date.

a. Funding: $ _80,440_

b. Number FTEGS: _1.5_

Total funding of the Parent Agreement and the number of FTEGS supported
the Parent Agreement during the current 12-month reporting period.

a. Funding: $ _83,277_

b. Number FTEGS: _1.0_

Total AASERT funding and the number of FTEGS and undergraduate students
5) supported by AASERT funds during the current 12-month reporting period.

a. Funding: $ _102,741.50 /3 years_

b. Number FTEGS: _1.0_

c. Number UGS: _0_

IFICATION STATEMENT: I hereby verify that all students supported by the
ERT award are U.S. citizens.

[signature]   _October 17, 1997_
ncipal Investigator   Date

X-ray Microbeam Mapping of Microtexture Related to Fatigue

Crack Asperities in Al-Li 2090

J.D. Haase, A. Guvenilir, J. R. Witt and S. R. Stock*

School of Materials Science and Engineering and

Mechanical Properties Research Laboratory

Georgia Institute of Technology

Atlanta, GA 30332-0245

ABSTRACT:

In certain orientations, Al-Li 2090 T8E41 cracks more slowly in fatigue than other aluminum alloys due to roughness-induced closure linked to the average texture or macrotexture. For this application, three-dimensional, non-destructive measurement of microtexture and strain evolution within samples was developed using synchrotron polychromatic x-ray microbeam diffraction [1-4]; its use in mapping the microtexture of fatigue crack asperities in Al-Li 2090 is the subject of this report. Groups of adjacent grains with nearly identical orientations are found at numerous locations in the plate centers, and this type of "mesotexture" appears closely tied to asperity formation. Changing arrangements of 111 diffraction spots relative to the samples' rolling and crack propagation directions are found to correspond to the transitions between a relatively planar section of the crack and an adjacent asperity.

---

*Author to whom all correspondence should be addressed. (street address: 778 Atlantic Drive, e-mail: stuart.stock@mse.gatech.edu)

INTRODUCTION:

Knowledge of the three-dimensional distribution of stress, strain, microtexture, etc. is sometimes necessary in order to understand the complex macroscopic behavior of today's engineering materials. More specifically, understanding the role of microtexture and the evolution of strain in response to monotonic and cyclic loading would lead to improved models for predicting a material's macroscopic behavior. One such method under development, three-dimensional microbeam x-ray diffraction tomography, is being used to investigate Al-Li 2090, an engineering alloy with interesting properties. In this alloy, fatigue crack growth rates along certain plate orientations are unusually low compared to those of other Al alloys [5,6]. This is related to a characteristic macrotexture (i.e., the texture averaged over a large number of grains) in the center of the plates which produces a rough, asperity dominated crack face and significant crack deflection [7]. The prominent macrotexture of the center of plates of this Al alloy has been correlated with the geometry of asperities on fatigue crack faces [7], but the role of microtexture on the path of fatigue cracks through the solid appears to have received little attention.

Orientation Imaging Microscopy (OIM) is an alternative to the microtexture mapping method used in this work, and it determines crystal orientation from the distribution of backscattered electrons in a scanning electron microscope or SEM [8,9]. The relatively shallow interaction volume of electrons prevents this method from examining the interior of bulk samples without destructive sample preparation. Another drawback of the OIM method is that it requires special sample preparation; for example, polishing damage must be removed. In contrast, the x-ray microbeams described below allow the sample's entire volume to be mapped nondestructively, an important advantage if the evolving strain accumulation ahead of the crack is also of interest.

The goal of the work reported here is to understand how local changes in the microtexture lead to the low fatigue crack growth rate in Al-Li 2090. To this end, transmission Laue patterns using synchrotron x-ray microbeams were recorded at numerous positions on a compact tension sample. The commissioning of the new high brightness sources ESRF (European Synchrotron Radiation Facility) and

APS (Advanced Photon Source) have stimulated others to employ similar approaches to mapping microtexture [e.g., 10,11]. Emphasis in this paper is on identifying what features or changes in features within the diffraction patterns correlate asperity formation. In other words, the approach is to determine the location and orientation of individual grains or groups of similarly aligned grains related to asperity formation in Al-Li 2090. Comparison of the observed microtexture associated with a particular large asperity and the macrotexture of Al-Li 2090 demonstrates the present results are consistent with earlier reports.

BACKGROUND:

One result of the crack face roughness in Al-Li 2090 is crack closure, the phenomenon where the crack faces come into contact prematurely during unloading of the sample (i.e., before the minimum stress of a fatigue cycle is reached) or where the crack faces remain in contact much longer than expected during loading [12]. Crack closure, in combination with significant crack deflection which increases the total crack length, leads to a reduced driving "force" for crack propagation and lower fatigue crack growth rates [13].

In 12.7 mm thick plates of Al-Li 2090 T8E41, the macrotexture of the center of the plate is very different from that in the outer sections [7], and the surfaces of fatigue cracks are much rougher, with larger, steeper asperities in the center than in the outside of the plate. The center region texture is characterized by two strong preferred orientations {123}<634> and {110}<112> and one weak preferred orientation {112}<111>; and Yoder *et al* [7] have shown that the orientations of the faces of the asperities are related to this macrotexture. Using the macrotextural information contained in pole figures, it was determined that the angle between the two faces of large asperities corresponds to that between high density {111} orientations in the pole figure. Thus, the shape of asperities is a direct consequence of the macrotexture.

Given that the morphology of the crack surface relates to the macrotexture present, the question remains: whether asperities in the center of plates of Al-Li 2090 form at random within the volume of material through which the crack is constrained to grow (by the notch) or whether variation in microtexture within this volume dictates where large and small asperities develop. In other words, does the crack choose its path to avoid grains or groups of grains with certain orientations or to grow through individual grains, groups of grains or specific orientations of grain boundaries. The resulting large crack deflections and accompanying fatigue crack closure, which has been measured macroscopically [5,6] and with high resolution x-ray computed tomography [14-16], are responsible for the very low fatigue crack growth rates in the L-T orientation. Side-grooves can minimize crack deflection (Fig.1a), but very large deflections are the rule otherwise (Fig. 1b).

EXPERIMENTS:

Compact tension samples were examined in this study of microtexture: identification of the microtexture producing crack deflection and asperity formation in Al-Li 2090 requires examination of samples with geometries that can be compared with those of other investigators. The compact tension samples had a thickness of 2.7 mm and were machined from the center of plates of Al-Li 2090 T8E41; the specific dimensions are discussed elsewhere [16,17], but the scaling was in accordance with ASTM E-399-83 [18]. Fatigue cracks were grown in L-T oriented compact tension samples (i.e., loading along the L direction and crack propagation along the T direction) with R = 0 .1 (i.e., $\sigma_{min}/\sigma_{max}$), 5 Hz frequency and haversine wave form. Most of the samples tested to date had side grooves which minimized crack deflection and allowed valid comparisons to be made with other's observations of stress intensity range, etc. A number of samples were examined before crack propagation, several were examined after fatigue cracks had extended 6-7 mm and a few specimens were studied after fracture. This report focuses on the samples which were fractured.

In the fractured samples, the volume of material adjacent to the crack was cut from the sample so that the specimen could be examined in the transmission parallel to the rolling direction (L) (Fig. 2). With sample thicknesses (along L) greater than 3mm, the number of overlapping diffraction streaks made analysis difficult and required impractically long exposure times.

The microtexture was mapped in the various compact tension specimens by translating the sample along the two orthogonal axes perpendicular to the beam by fixed increments and recording the resulting transmission Laue pattern. Prior to microbeam data collection, the surfaces of the fractured compact tension samples were viewed optically to locate asperities so that microtexture data collection could concentrate on areas of interest. For the fractured compact tension specimens, most of the Laue patterns were recorded with the incident beam parallel to the rolling direction (L). In this "parallel" geometry (Fig. 2), the beam was translated along the short transverse (S) direction for various positions along the transverse (T) axis. The fractured compact tension specimens were also examined with the incident beam parallel to the short direction (i.e., perpendicular to the face of the plate and in the "perpendicular" geometry) in order to investigate whether asperities could be located in unfractured, unsectioned compact tension specimens. In samples where both fracture surfaces are available, matching locations on each face were studied with the x-ray microbeams.

All diffraction data were collected with polychromatic bending magnet radiation at Stanford Synchrotron Radiation Laboratory (SSRL) beamline 2-2 (3.0 GeV, beam currents between 20 and 100 mA). Pinhole collimators with 100, 30 or 10 µm diameters have been used. Exposure levels were on the order of 2×10^3 and 1×10^4 mA·sec for the 100 and 30 mm collimators, respectively. The collimator was placed 55 cm from the sample in order to minimize the effect of scatter from the edges of the pinhole. The ~20 arcseconds of vertical divergence of the beam was enough to broaden the beam from the 10 µm diameter collimator to 80 µm vertically at the sample position. Image storage plates [19,20] were used to record the polycrystalline Laue patterns. Initially, 20 x 25 cm plates were read with 100 µm pixel size

and 1024 levels of contrast in a Fuji BAS-2000 Imaging Plate Scanner. Once a Fuji BAS-2500 Imaging Plate Scanner became available, all data was collected on this system on plates with an area of 20 x 40 cm and read with 50 μm pixel resolution and 256 levels of contrast. Additional levels of contrast could be obtained in the BAS-2500 system at the cost of much larger data file sizes, but 256 levels of contrast provided adequate range for these experiments. In some of the patterns, a filter with an absorption edge in the wavelength range of interest was placed before the collimator in the beam in order to introduce a sharp change in contrast in the polycrystalline diffraction pattern [21]. The use of a filter allows one to index the pattern (Fig. 3).

RESULTS AND DISCUSSION:

In the fractured compact tension specimens, the thickness was chosen so that the number of grains in the beam path along the rolling direction (i.e., in the parallel diffraction geometry) would be minimized. The appearance of complex streaks is evident in microtexture mapping in the parallel geometry and greatly complicated the process of determining the orientation of specific diffracting regions. Since the grain size in Al-Li 2090 along the L direction is on the order of 1 mm and along the S direction is on the order of 50 μm, diffraction patterns from the samples would be expected to consist of streaks from several grains, but not several tens of grains. The separation between sampling positions was chosen so that streaks from each grain would be present in more than one diffraction pattern (i.e., to reveal gradual changes in microtexture) and ranged from 20 to 100 μm. Grouping of 111 streaks is observed in both the parallel and perpendicular geometries, and this suggests that results obtained in the two experimental geometries can be correlated. This is important since the parallel geometry allows straight-forward diffraction pattern interpretation and beam position correlation with asperity locations determined by scanning electron or optical microscopy.

Figure 4 juxtaposes a map of microbeam positions and an SEM micrograph of the fracture surface viewed along the loading axis (i.e., normal to the nominal fracture plane). One side groove is

visible at the top of the micrograph, and the crack propagated from left to right. The very large asperity described below lies adjacent to the side groove and extends almost the entire length of the micrograph. Identifying specific streaks or clusters of streaks associated with asperities in the perpendicular geometry is much more difficult without the guidance of the results of mapping in the parallel geometry.

Figure 5 shows the same area of the sample as Fig. 4, but the sample is viewed at a large angle of tilt. The white dashed line indicates the position of a scan of the beam along the sample's S direction. Note the large asperity at the top of the SEM micrograph. The center portions of two diffraction patterns are shown to the right of the fractograph, and the arrows indicate the position where each was recorded. In Fig. 3 and Figs. 5 - 9, the diamond at the center of each Laue pattern is a lead beam stop whose thickness was chosen to attenuate most (but not all) of the incident beam; and increasing diffracted intensities are indicated by the darkening of the pattern. The abrupt change of texture at the edge of the asperity is seen by the quite pronounced change in 111 streak position to the right of the beam stop. Within the volume of asperity, the orientation of the 111 streaks varied little from the upper pattern of Fig. 5. Outside the asperities, the 111 streaks either had different orientations or were not present.

A series of diffraction patterns in the parallel geometry and spanning the asperity along the S direction of the sample is shown in Fig. 6. Only the central portion of the patterns are shown, and the difference in diffraction patterns taken from the asperity volume are easily seen compared to those of nearby planar regions of the crack face. This type of mapping allows one to map out the entire asperity along both the S and T direction. Figure 7 shows a series of diffraction patterns taken in the same geometry but with the translation between exposures being along the sample's T direction (i.e., along the length of the asperity). The microtexture revealed by the 111 streaks change little over the 250 μm of translation.

Figure 8 shows a series of diffraction patterns of the same asperity shown in Fig. 7 but recorded in the perpendicular geometry (i.e., with the incident x-ray beam parallel to the S direction and normal to

the face of the plate). The positions of diffraction patterns in Fig. 8 are separated by 20 μm translations along the sample's T direction. This demonstrates that the microtexture producing the 111 streaks parallel to or nearly parallel to the plate's T direction in the parallel diffraction orientation also can be unambiguously seen in the perpendicular geometry as horizontal 111 streaks. It is likely, therefore, that volumes of material with the proper microtexure to form asperities can be located nondestructively in samples prior to crack growth. Whether or not such volumes of material actually form asperities or significant crack deflection, however, depends on many other factors, including whether the advancing crack will intersect the volume.

It is also important to ascertain whether the microtexture inside and outside of the asperity described above is consistent with the expected average texture. Figure 9 shows an experimental 111 pole figure (after [7]) from the central portion of plates of Al-Li 2090 T8E41. The section of the diffraction patterns just inside and just outside the asperity (Fig. 5) are reproduced, and the arrows link the diffraction patterns with the orientation in the pole figure producing the characteristic streaks. Seeing that these orientations produce exit beams in the proper directions and with the proper diffraction angles requires locating the entrance and diffracted beams (S_0 and S_{111}, respectively) coplanar with and at an angle $\pi/2$ - θ_B from the plane normal. Consider the solid rectangle in the right portion of the pole figure as an idealized representation of orientations comprising this portion of the macrotexture, and note that the top and bottom of this region represent those orientations which will produce diffraction streaks at the greatest angle with respect to the transverse direction. Since S_0 is along L for the diffraction patterns shown to the right of the pole figure, constructing a stereographic projection with the reference direction along L (shown below the pole figure) allows straight-forward comparison. The rectangle in the pole figure rotates to the position shown and exit beams S_{111} corresponding to the inner-most corners of the solid rectangles are indicated by the dashed lines leading to the outermost corners of the open triangles (on the back of the projection). From this representation of the texture, one expects 111 streaks to be at an angle no greater than $\pm$ 25° from T; experimentally the angles are ~ +20° in the upper pattern and ~-

25°in the lower pattern. Note that there will be a spread of Bragg angles observed, and 90 - θ_B will be 80° for the innermost corner of the rectangle in the stereographic projection. This Bragg angle (10°) corresponds to diffraction of a wavelength of 0.812 Å, and the rest of the grains with 111 orientations represented by the rectangle are expected to diffract at shorter wavelengths. When the molybdenum filter is inserted in to the beam, the position of its K-edge (0.62Å) intersects the 111 streaks near the transverse direction in some of the diffraction patterns, and this confirms the identification of the portion of the macrotexture related to the microtexture inside and outside of the asperity.

A consistent picture emerges of the relationship between microtextrue, macrotexture, asperity formation and "choice" of crack path of the central portion of plates of Al-Li 2090 T8E41. Groups of adjacent, highly-oriented, plate-like grains form near-single-crystal regions within the plate, and this spatial distribution of microtexture is a specific type of mesotexture which defines favored crack paths. In other words, macrotexture describes large-scale average texture (e.g., an average over the sample), microtexture is used to describe the orientations present at the subgrain scale or in a grain-by-grain average and mesotexture is used to the average prefered orientation over an assembly of adjacent grains. The present observations are consistent with the distribution of misorientation angles measured across grain boundaries for this material [22]. The data presented above suggest that fatigue cracks tend to propagate crystallographically within or adjacent to these highly-oriented volumes and that crack deflection is likely at the boundary of such a region. The relatively high probability that adjacent pancake-shaped grains are nearly aligned leads one to expect fracture features with aspect ratios and orientations similar to that of the individual grains. The correlation between macrotexture and the {111} faces of asperities is therefore not surprising. Near-single-crystal regions consisting of multiple grains will tend to act like single crystals, slip across grain boundaries within this region will relatively easy and the resulting fracture surface will be crystallographic with {111} faces. Thus, the spatial distribution of

these highly-oriented regions appears to govern whether or not asperities are present on fatigue crack surfaces in this alloy / heat treatment and where on the surfaces these asperities form.

The observation of mesotexture is consistent with the very low fatigue crack growth rates seen in Al-Li 2090 samples tested in the L-T orientation. Crystallographic crack propagation tends to be considerable slower that transgranular cracking [23]. Further, forcing the fatigue crack out of the nominal plane of the notch would also be expected to slow propagation rates since the area of the fatigue crack would be greatly increased, while the effective crack length would be unchanged. These factors, when coupled with decreased driving "force" from roughness induced crack closure, explain the unusually low fatigue crack growth rates in Al-Li 2090.

CONCLUSIONS:

The characteristic microtexture of Al-Li 2090 T8E41 that leads to the formation of asperities and crack closure in fatigue crack growth appears to be a specific type of mesotexture present in this material: sets of adjacent grains are so highly aligned that they may be regarded as nearly single crystalline volumes. A relationship between macrotexture and a specific asperity on the fatigue crack surface was identified. Thus, the size, shape and location of these asperities was shown to depend on microtexture, mesotexture, and macrotexture. When coupled with high resolution x-ray computed tomography observations of the crack face contact as a function of crack face geometry and stress intensity (in the interior of the samples) [14-17], the present observations complete the link between the orientation of individual grains / groups of adjacent grains, macrotexture, the formation of asperities, the positions where crack faces contact as a function of applied stress and macroscopic manifestations of the crack closure process in Al-Li 2090 T8E41. Further elaboration of details such as amount and spatial distribution of near-single-crystalline regions is needed before numerically realistic models may be assayed. Fortunately gathering such information is quite straight-forward with the x-ray microbeam techniques used in this work. The development of these x-ray microtexture mapping techniques is so

encouraging that it is not imprudent to suggest that it should be possible to non-destructively explore the three-dimensional microtexture within intact macroscopic samples of complex materials such as Al-Li 2090.

ACKNOWLEDGMENTS:

REFERENCES:

1. S.R. Stock, A. Guvenilir, D.P. Piotrowski, and Z.U. Rek, *MRS Symp. Proc.* **375**, p. 275 (1995).

2. D.P. Piotrowski, *Synchrotron Polychromatic X-ray Diffraction Tomography of Large Grained Polycrystalline Samples*, MS Thesis, Georgia Inst. of Technology. March 1996.

3. D.P. Piotrowski, S.R. Stock, A. Guvenilir, J.D. Haase, and Z.U. Rek, *MRS Symp. Proc.* **437**, p.125 (1996).

4. S.R. Stock, J.D. Haase, D.P. Piotrowski, J.R. Witt and A. Guvenilir, to appear in <u>Making and Using Small X-Ray Beams</u> *Eighth Users Mtg for the Advanced Photon Source*, (1997).

5. P.S. Pao, L.A Cooley, M.A. Imam and G.R. Yoder, *Scr. Met.* **23**, 1455 (1989).

6. K.T. Venkateswara Rao, W. Yu and R. O. Ritchie, *Met Trans.* **19A**, 549 and 563 (1988).

7. G.R. Yoder, P.S. Pao, M.A. Imam and L.A. Cooley, in *Proc. Fifth Int. Aluminum-Lithium Conf.*, T.H. Sanders, Jr. and E.A Starke, Jr., Eds, Mat. and Comp. Eng. Publ., Birmingham, UK p. 1033 (1989).

8. B.L. Adams, S.I. Wright and K. Kunze, *Met Trans*. **24A**, 819 (1993).

9. D.J. Dingley, *Scanning Electron Microscopy* **2**, 569 (1984).

10. H.F Poulsen, S. Garbe, T. Lorentzen, D. Juul Jensen, F.W. Poulsen, N.H. Anderson, T. Frello, R. Feidenhans'l and H. Graafsma, *J. Synchrotron Rad.* **4**, 147 (1997).

11. P.C Wang, G.S. Cargill III and I.C. Noyan, *MRS Symp. Proc.* **375**, p.247 (1995).

12. R.O.Ritchie, in *Fatigue Thresholds*, J. Backland, A. Blom and C.J. Beevers eds., Eng Advisory Services, Warley, UK, p. 503 (1981).

13. R.O.Ritchie, *Mater. Sci. and Eng.* **103**, 15-28 (1988).

14. T.M. Breunig, S.R. Stock, S.D. Antolovich, J.H. Kinney, W.N. Massey and M.C. Nichols, *ASTM STP,* **1131,** 749 (1992).

15. A. Guvenilir, T.M. Bruenig, J.H. Kinney and S.R. Stock, *Acta. Mat.* **45,** 1977 (1997).

16. A. Guvenilir, *Investigation into Asperity Induced Closure in an Al-Li Alloy Using X-Ray Tomography*, PhD Thesis, Georgia Inst. of Technology. December 1995.

17. A. Guvenilir, S.R. Stock, M.D. Barker, and R.A. Betz, in *4th Int. Conf. On Aluminum Alloys,* T.H. Sanders, Jr. And E.A. Starke, Jr., Eds., Georgia Institute of Technology, Atlanta, p.   (1994).

18. ASTM Standard E-399-83.

19. Y. Ameniya, T. Matsushita, A. Nakagawa, Y. Satow, J. Miyahora and J. Chikawa, *Nucl. Instrum. Meth.* **A266**, 645 (1988).

20. B.R. Whiting, J.F. Owen and B.R. Rubin, *Nucl. Instrum Meth.* **A266**, 628 (1988).

21. S.R. Stock, Z.U. Rek, Y.H. Chung, P.C. Huang, and B.M. Ditchek, *J Appl Phys*, **73**, 1 (1993).

22. F. Barlat, S.M. Miyasota, J. Liu and J.C. Brem, in *4th Int. Conf. on Aluminum Alloys*, T.H. Sanders, Jr. And E.A. Starke, Jr., Georgia Institute of Technology, Atlanta, p. 389 (1994).

23. S. Suresh Fatigue of Materials Cambridge University Press, Cambridge UK, 1991.

Figure 1. Crack profiles on the faces of Al-Li 2090 compact tension samples: that on one face is shown in black and on the other in gray. The crack profile at both faces of the grooved sample (CT-2) is shown in (a) while (b) shows the crack path on the front and back surface a sample without side grooves (CT 31). The notch tip is at the left.

Figure 2. Experimental geometry with incident x-ray beam parallel to the rolling direction (L). The transverse plate direction T is horizontal. The sample is a section from a fractured compact tension of Al-Li 2090. Incident and exit beams are shown, and the diffracted beams exit the fracture surface.

Figure 3. Two diffraction patterns at the same location on compact tension sample CT21. These patterns were recorded in the perpendicular geometry, (i.e., along the short plate direction), the transverse plate direction T is horizontal. A 10 μm diameter collimator was used to form the microbeam, and the pattern on the right was made by placing a 75 μm thick molybdenum filter in the incident beam path. The presence of this filter causes a sharp change in contrast for diffraction of wavelengths above and below 0.62 Å, i.e, at the wavelength of the Mo K-edge. The darker the pixel value in this figure, the greater the diffracted intensity. The white diamond in the center of the pattern is the beamstop and, by design, the incident beam penetrates it. The separation between the exit surface of the sample and the detector was approximately 245 mm

Figure 4. Map of microbeam position (top) at the same scale as the SEM fractograph (bottom) of compact tension sample CT21 containing the large asperity described in the text and in Fig. 5-8. The viewing perpective is normal to the surface, the crack propagated from left to right and one of the side grooves appears at the the top of the micrograph.

Figure 5. SEM fractograph of the region of the compact tension sample shown in Fig. 4 but at a high angle of tilt. The large asperity appears at the top, and the dashed line marks the line along which the microbeam was scanned. The central portion of diffraction patterns just within (top right) and just outside (bottom right) the asperity are shown to the right of the fractograph; the two positions are identified by the arrows. The darker the pixel value in these diffraction patterns, the greater the diffracted intensity. The white diamond in the center of the pattern is the beamstop. These diffraction patterns were recorded with a separation of about 245 mm between the exit surface and the detector.

Figure 6.   A series of five diffraction patterns showing the characteristic change in microtexture in and around an asperity in CT21. The images were taken in 50 µm translation steps with a 10 µm diameter collimator beam and translation along the short rolling direction (S) across the asperity. The sample was oriented so that the incident x-ray beam is parallel to the rolling direction. Pattern b through d are from the asperity region, and the gray scale and sample-detector separation are the same as in Fig. 5.
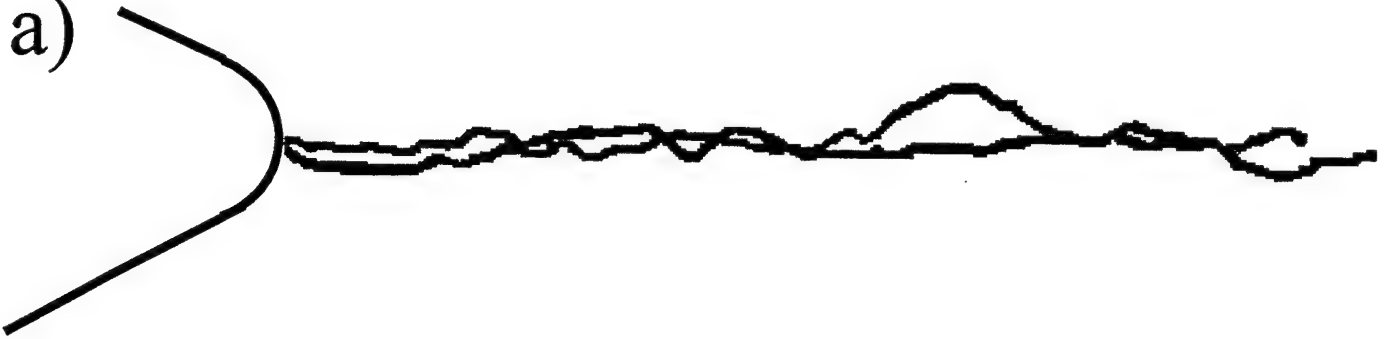
Figure 7.   A series of five diffraction patterns recorded with the 10 µm diameter collimator and showing the <111> streaks comprising the characteristic change in microtexture from an asperity region. The images are from positions within the asperity separated 50 µm apart along the transverse rolling direction (T), and the gray scale and sample-detector separation are the same as in Fig. 5.

Figure 8.   Portions of perpendicular geometry diffraction patterns recorded at five different positions along the length of an asperity. This asperity was also shown in Fig. 6 and 7. Translation was in 20 µm steps along the plate's T direction and the 111 streaks lie along this direction. A 10 µm diameter collimator was used to form the microbeam.

Figure 9.   Orientation of 111 diffraction streaks related to the macrotexture of the center of plates of Al-Li 2090 T8E41. The 111 pole figure (after [7]) is shown in the upper left, and the portion of the macrotexture producing the 111 streaks associated with the asperity is represented schematically by the solid rectangle in the right side of the pole figure. The centers of two diffraction patterns show the 111 streaks just outside (top right) and inside the asperity (lower right). The L-oriented stereographic projection (lower left) is used to relate the experimentally observed 111 streaks to the macrotexture: the locus of expected diffracted beam directions (i.e., the streaks) from the orientations within the solid rectangle are indicated by the elongated triangles nearly parallel with the T axis.
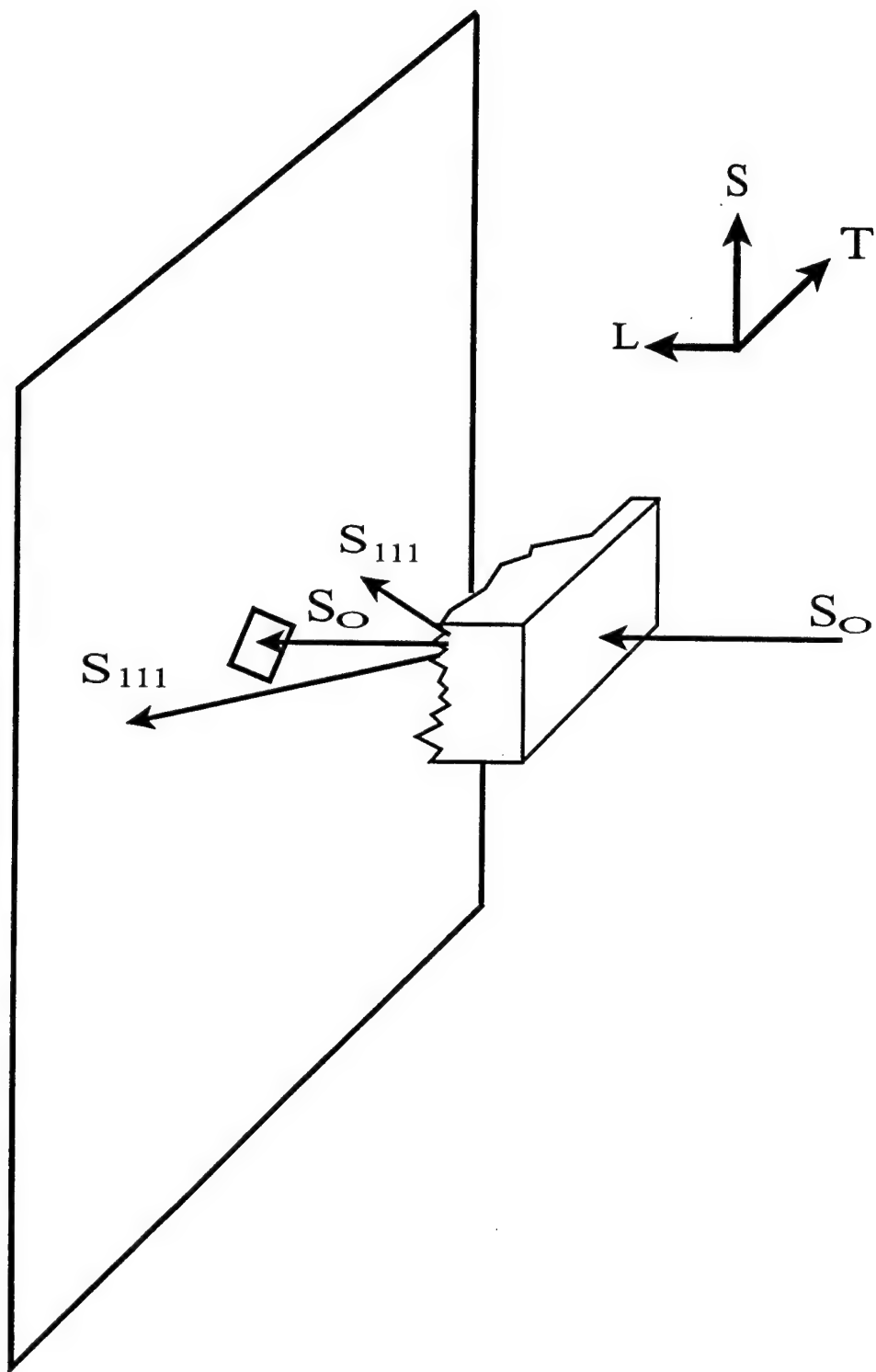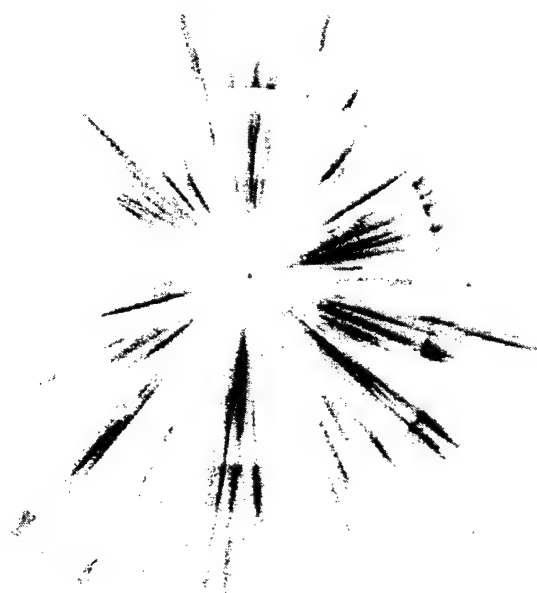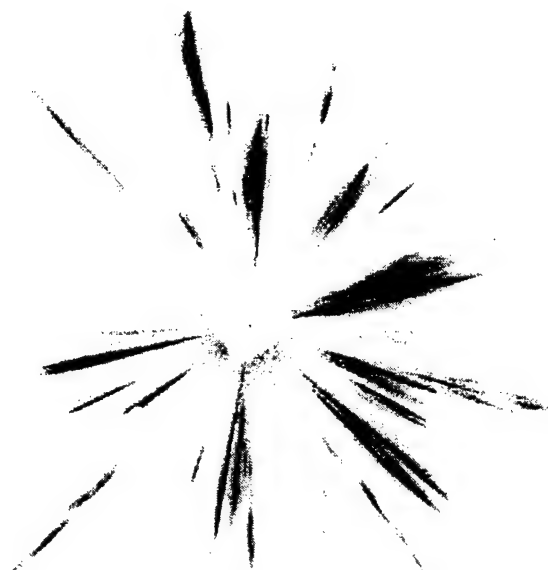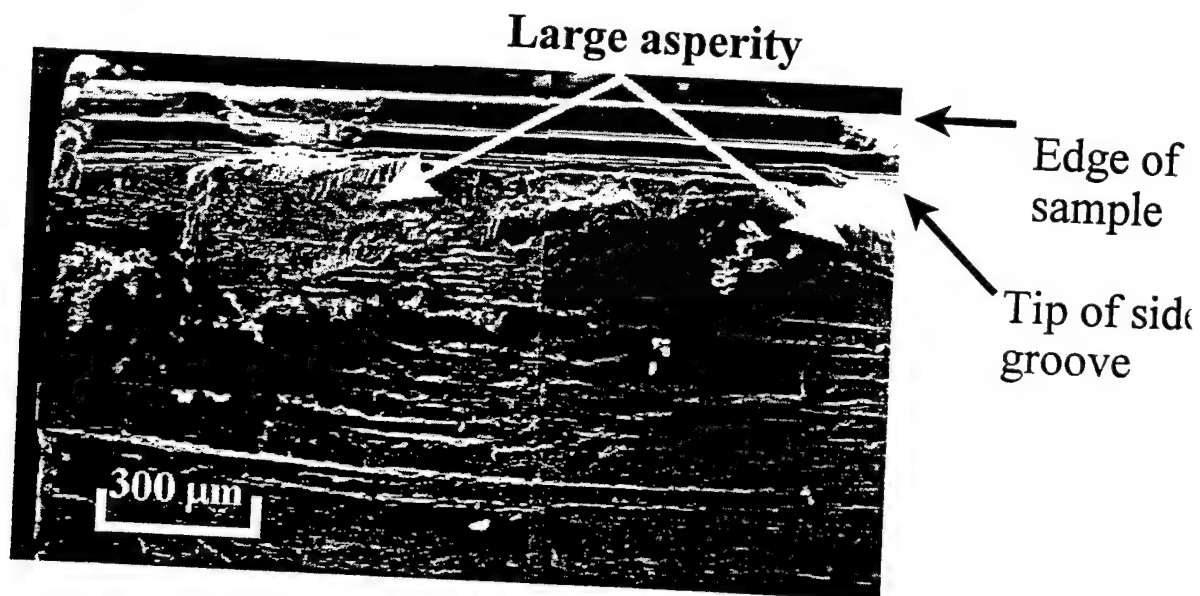
5 mm

a)

b)

200 mm

Y (μm)   300   500   800   1000   1200

X (μm)   0,0

75

200

Tip of side
groove

S

L

T

Large asperity

Edge of
sample

Tip of side
groove

300 μm

S

L

T

500 μm

100 mm

a)

50 mm

b)

c)

S

L

T

d)

e)

a)

50
mm

b)

c)

d)

e)

S

L

-T

S₀

S₁₁₁

π/2 − θ_B

~25°

L

T

S

100 mm

S

L

T
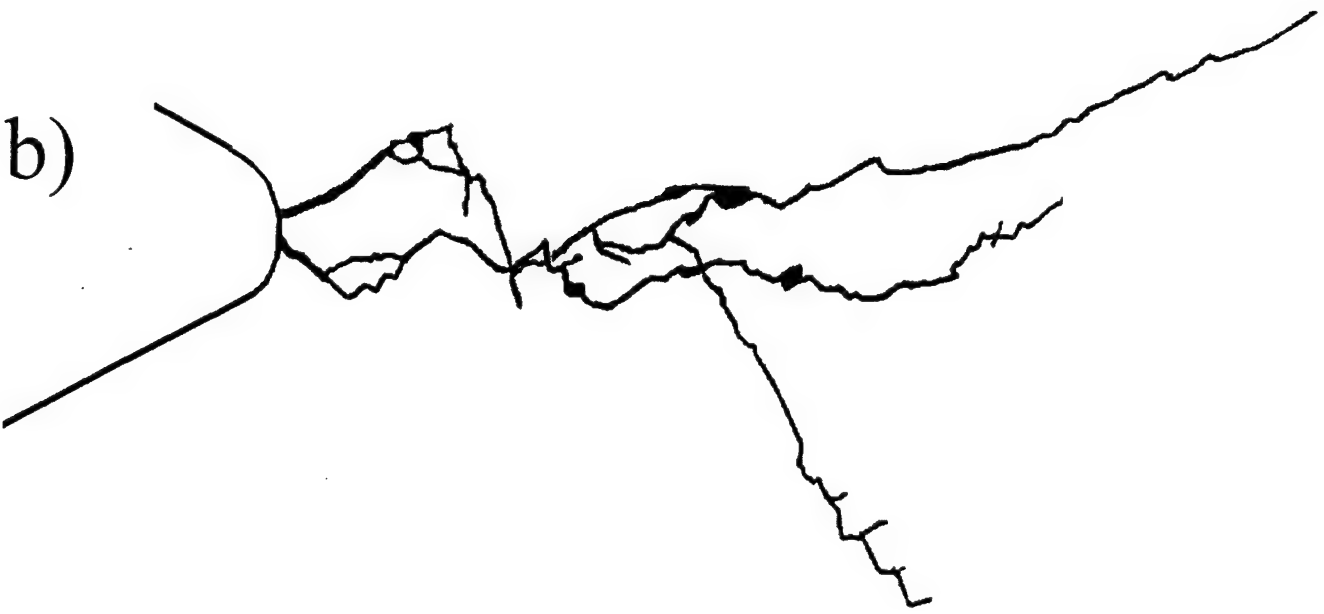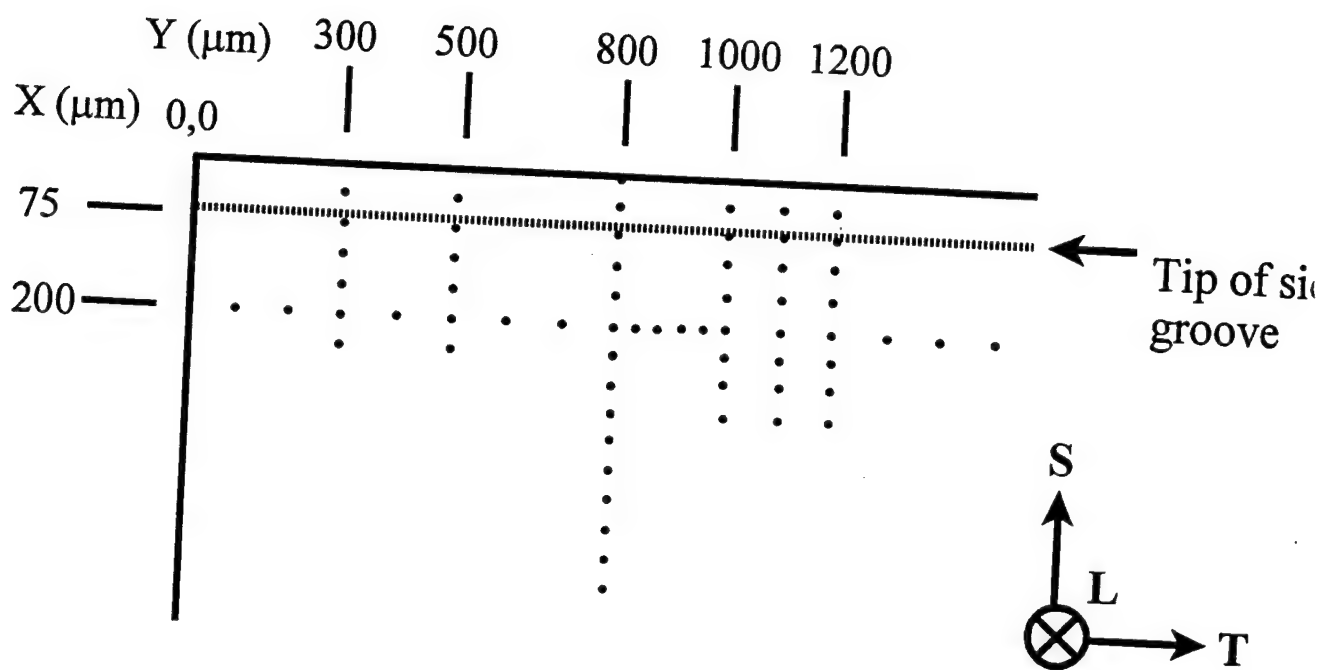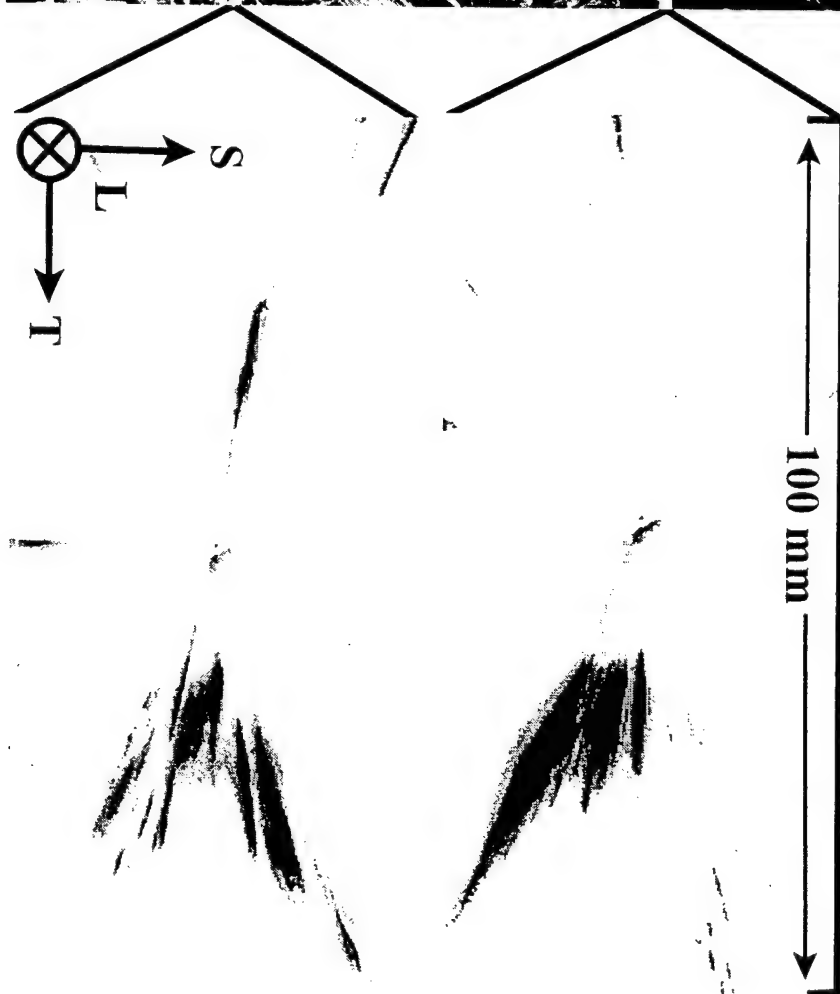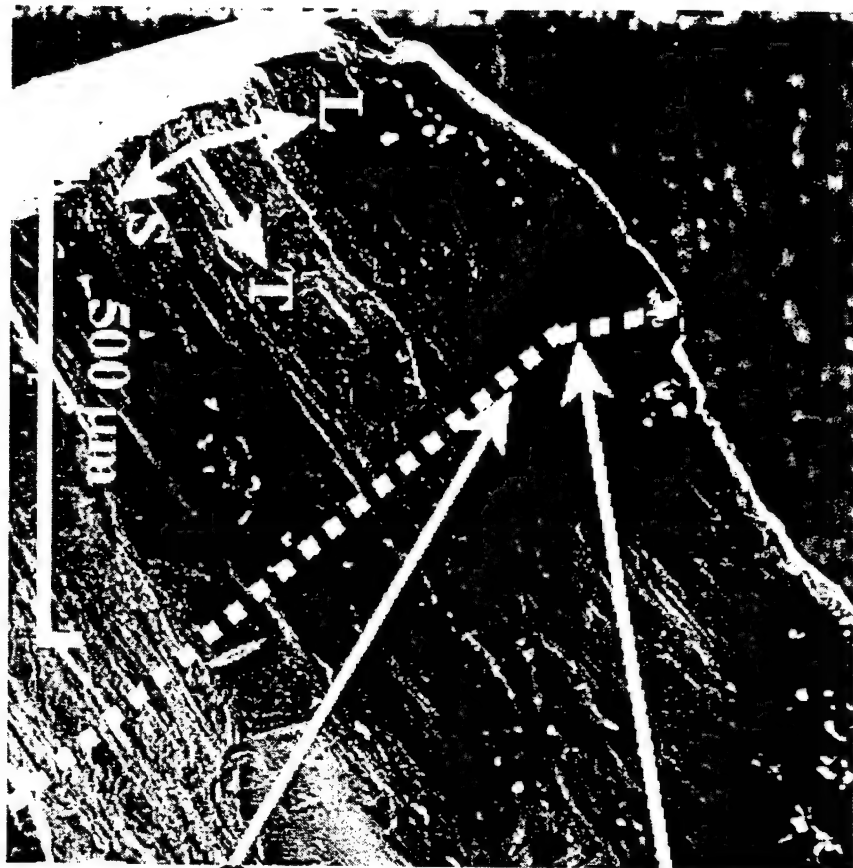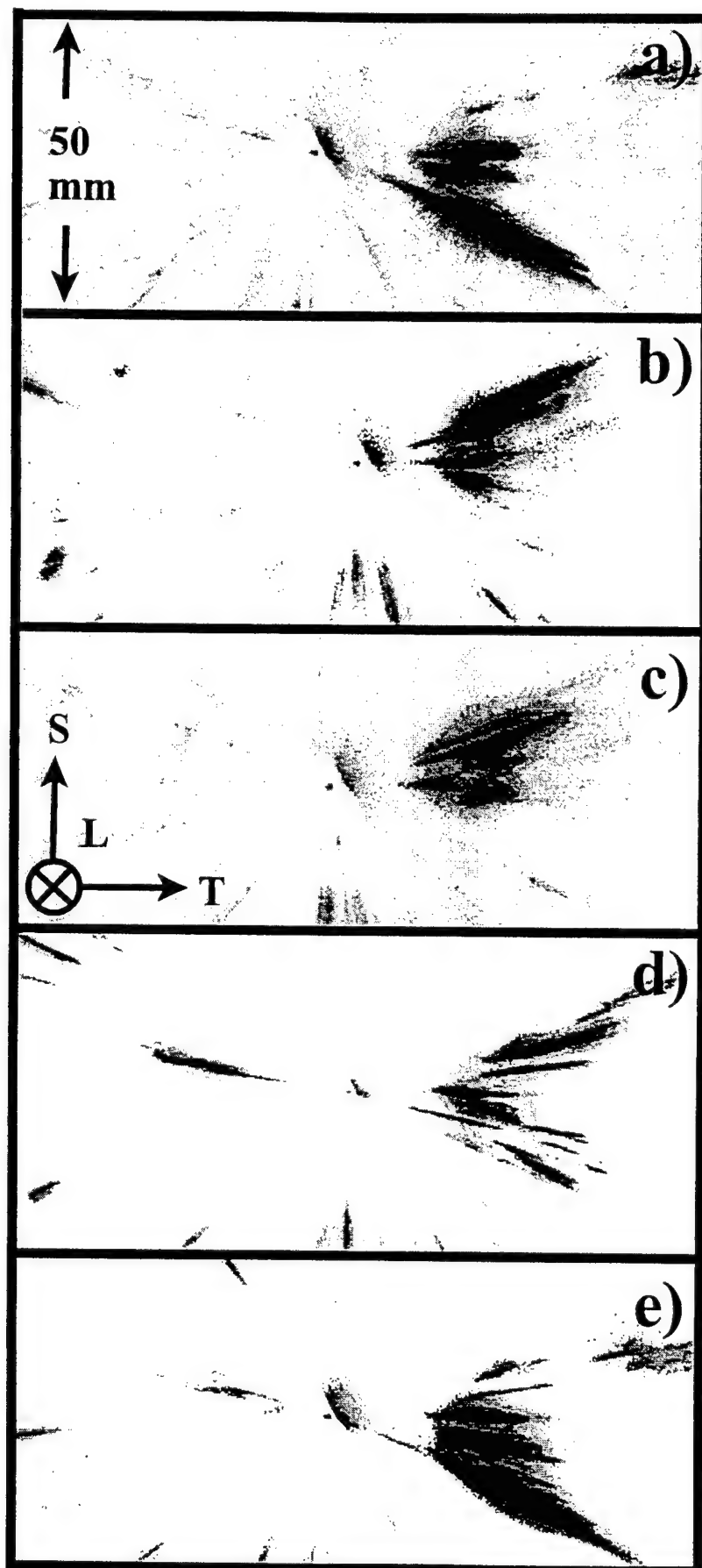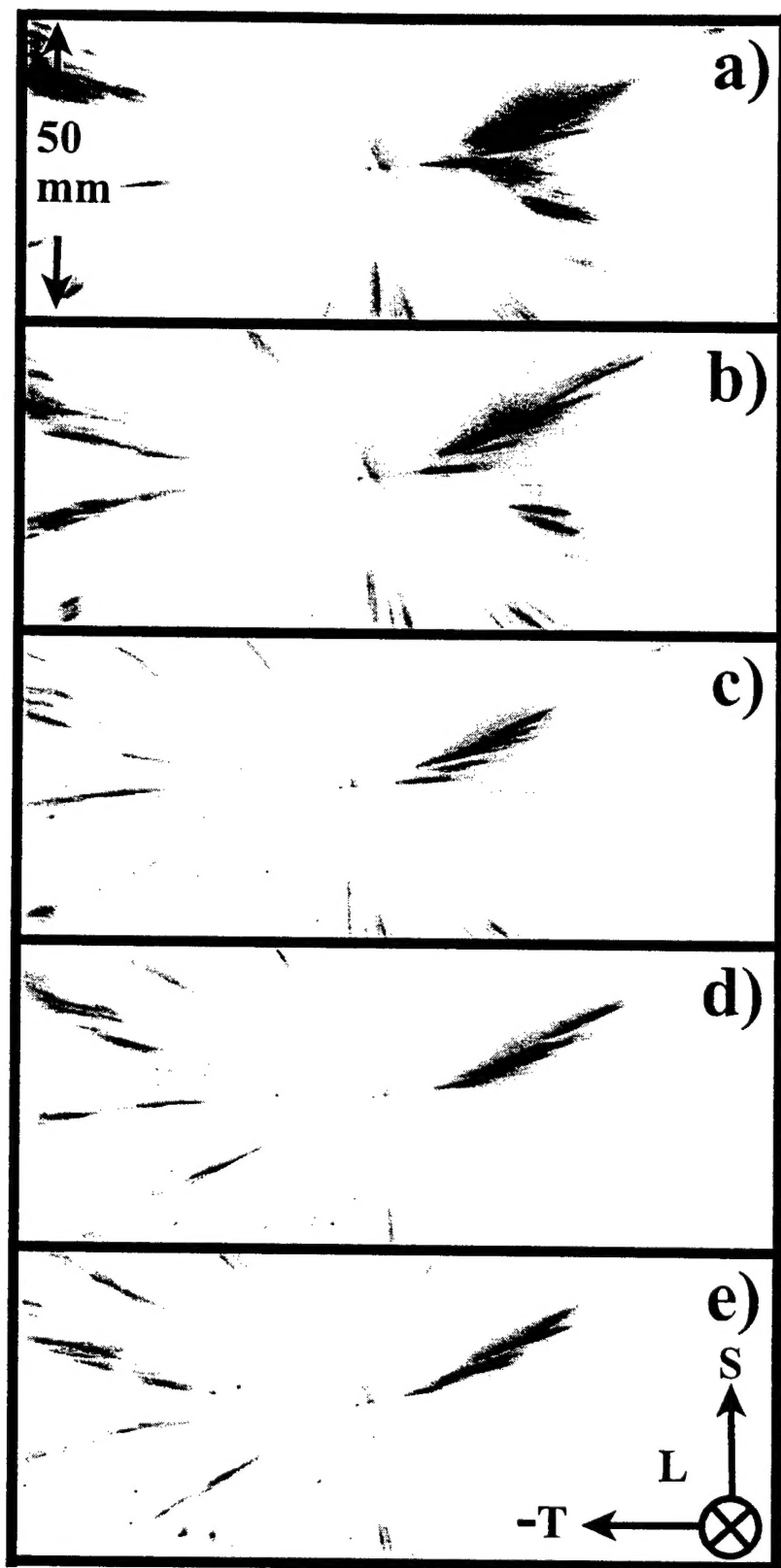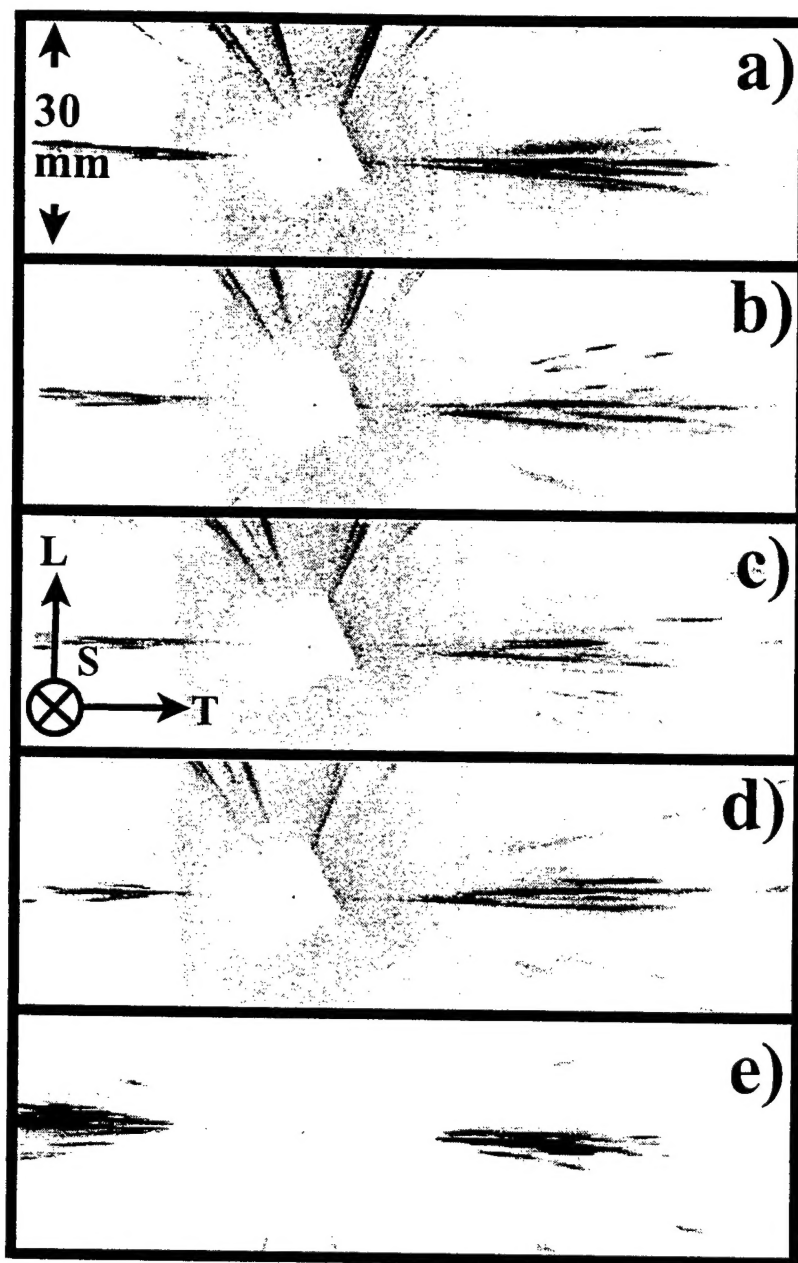
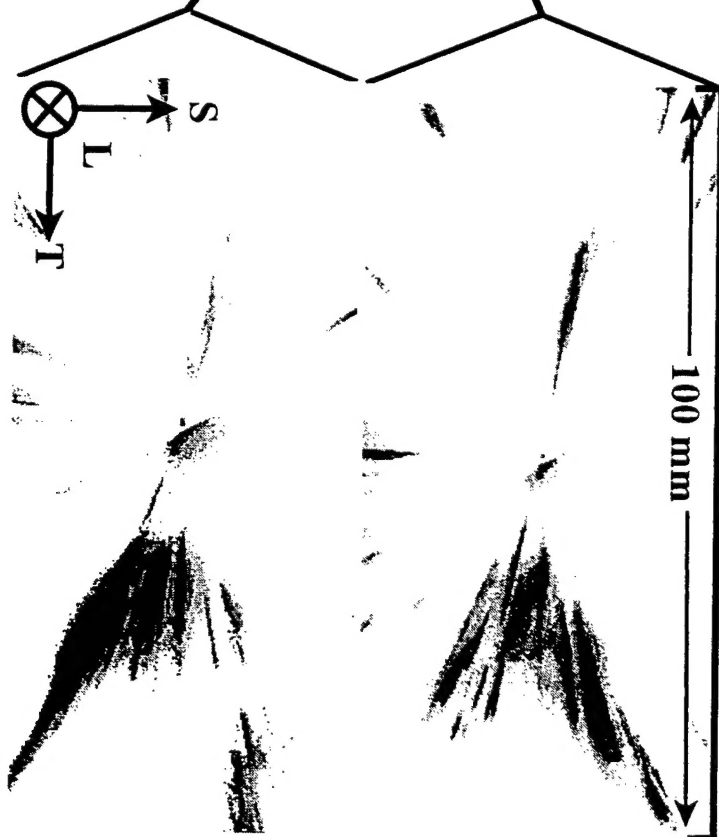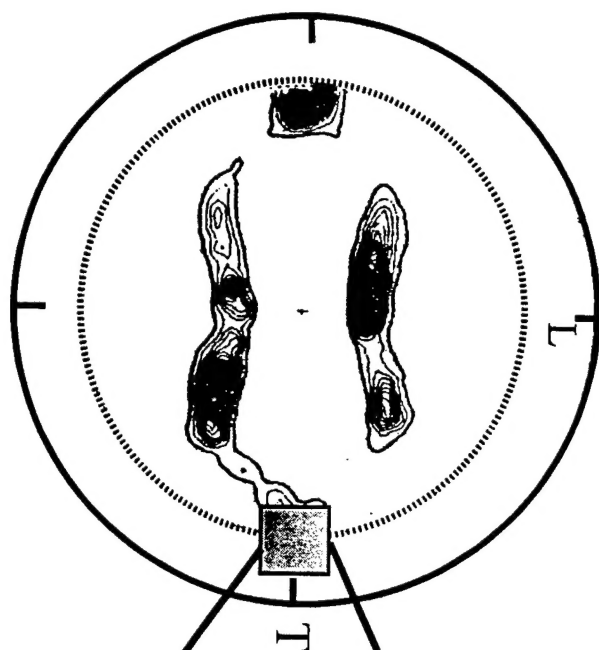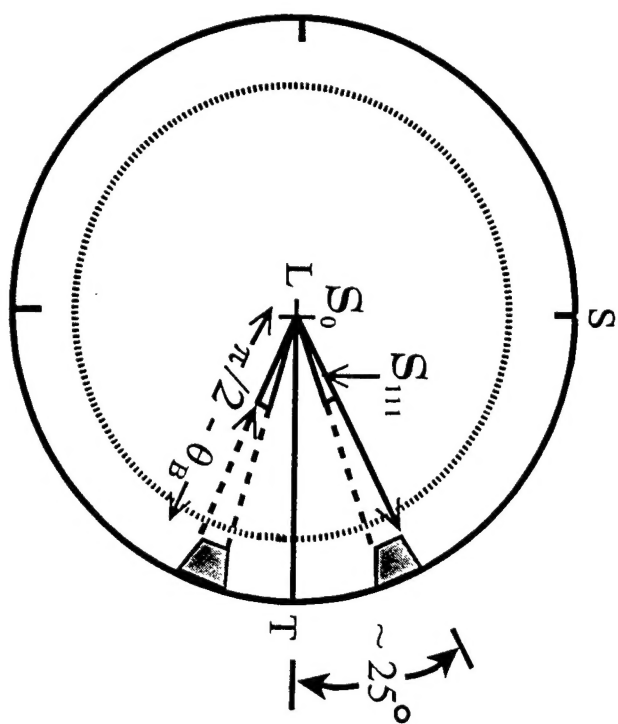# REPORT DOCUMENTATION PAGE

Public reporting burden for this collection of information is estimated to average 1 hour per response, including the time for reviewing instructions, searching existing data sources, gathering and maintaining the data needed, and completing and reviewing the collection of information. Send comments regarding this burden estimate or any other aspect of this collection of information, including suggestions for reducing this burden, to Washington Headquarters Services, Directorate for Information Operations and Reports, 1215 Jefferson Davis Highway, Suite 1204, Arlington, VA 22202-4302, and to the Office of Management and Budget, Paperwork Reduction Project (0704-0188), Washington, DC 20503.

1. AGENCY USE ONLY (Leave blank)	2. REPORT DATE Oct 17, 1997	3. REPORT TYPE AND DATES COVERED Final 7/1/96-9/30/97

4. TITLE AND SUBTITLE	5. FUNDING NUMBERS
Nondestructive 3 - Dimensional	N00014-94-1-0726

6. AUTHOR(S)

Stuart R. Stock

7. PERFORMING ORGANIZATION NAMES(S) AND ADDRESS(ES)	8. PERFORMING ORGANIZATION REPORT NUMBER
Stuart R. Stock, School of Mat. Sci & Eng., Georgia Institute of Technology 778 Atlantic Drive, Atlanta, GA 30332-0245	E18-X02 Line 4

9. SPONSORING / MONITORING AGENCY NAMES(S) AND ADDRESS(ES)	10. SPONSORING / MONITORING AGENCY REPORT NUMBER
George R. Yoder/Code 331, ONR, Ballston Tower One, 800 N. Quincy St., Arlington, VA 22217-5660	Met00a1---01

11. SUPPLEMENTARY NOTES

8. DISTRIBUTION / AVAILABILITY STATEMENT	12. DISTRIBUTION CODE
Unlimited	

13. ABSTRACT (Maximum 200 words)

Sychrotron X-ray microbeams were used to characterize the three-dimensional distribution of microtexture associated with asperity formation during fatigue crack propagation in Al-Li 2090 T8E41. Nondestructive techniques were developed, and beams formed by a 10 μm diameter collimator were applied. Focus was on the center portion of 12.5mm thick plates where macrotexture correlates with asperity geometry. A very distinct type of mesotexture was found: multiple adjacent grains have nearly identical orientations and form substantial volumes of near-single-crystal (NSC) material. Transitions between differently oriented NSC volumes or an NSC region and more randomly oriented grains seem to bound asperities.

14. SUBJECT TERMS Aluminum, Crack, Nondestructive, Microtexture, X-ray, Diffraction, Synchrotron Radiation Fatigue			15. NUMBER OF PAGES
			16. PRICE CODE

17. SECURITY CLASSIFICATION OF REPORT	18. SECURITY CLASSIFICATION OF THIS PAGE	19. SECURITY CLASSIFICATION OF ABSTRACT	20. LIMITATION OF ABSTRACT
Unclassified	Unclassified	Unclassified	Unlimited

Standard Form 298 (Rev. 2-89)
Prescribed by ANSI Std. 239-18
298-102

and Address(es). Self-explanatory.

Block 10. Sponsoring/Monitoring Agency Report Number. (If known)

Block 11. Supplementary Notes. Enter information not included elsewhere such as: Prepared in cooperation with...; Trans. of ...; To be published... When a report is revised, include a statement whether the new report supersedes or supplements the older report.

information, stamp classification on the top and bottom of the page.

Block 20. Limitation of Abstract. This block must be completed to assign a limitation to the abstract. Enter either UL (unlimited) or SAR (same as report). An entry in this block is necessary if the abstract is to be limited. If blank, the abstract is assumed to be unlimited.